

# Natural products as DNA methyltransferase inhibitors: a computer-aided discovery approach

Jose L. Medina-Franco · Fabian López-Vallejo · Dirk Kuck · Frank Lyko

Received: 9 April 2010 / Accepted: 20 July 2010 / Published online: 10 August 2010  
© Springer Science+Business Media B.V. 2010

**Abstract** DNA methyltransferases (DNMTs) represent promising targets for the development of unique anticancer drugs. However, all DNMT inhibitors currently in clinical use are nonselective cytosine analogs with significant cytotoxic side-effects. Several natural products, covering diverse chemical classes, have indicated DNMT inhibitory activity, but these effects have yet to be systematically evaluated. In this study, we provide experimental data suggesting that two of the most prominent natural products associated with DNA methylation inhibition, (–)-epigallocatechin-3-gallate (EGCG) and curcumin, have little or no pharmacologically relevant inhibitory activity. We therefore conducted a virtual screen of a large database of natural products with a validated homology model of the catalytic domain of DNMT1. The virtual screening focused on a lead-like subset of the natural products docked with DNMT1, using three docking programs, following a multistep docking approach. Prior to docking, the lead-like subset was characterized in terms of chemical space coverage and scaffold content. Consensus hits with high predicted docking affinity for DNMT1 by all three docking programs were identified. One hit showed DNMT1 inhibitory activity in a previous study. The virtual screening hits were located within the biologi-

cal-relevant chemical space of drugs, and represent potential unique DNMT inhibitors of natural origin. Validation of these virtual screening hits is warranted.

**Keywords** Cancer · Curcumin · DNA methylation · Drug discovery · EGCG · Natural product database · Virtual screening

## Abbreviations

DNMT	DNA methyltransferase
EGCG	(–)-epigallocatechin-3-gallate
HBA	Hydrogen bond acceptor
HBD	Hydrogen bond donor
MOE	Molecular operating environment
MW	Molecular weight
NCI	National Cancer Institute
RB	Rotatable bond
SAH	S-adenosyl-L-homocysteine
SAM	S-adenosyl-L-methionine
SP	Standard precision
TPSA	Topological polar surface area
XP	Extra precision

**Electronic supplementary material** The online version of this article (doi:10.1007/s11030-010-9262-5) contains supplementary material, which is available to authorized users.

J. L. Medina-Franco (✉) · F. López-Vallejo  
Torrey Pines Institute for Molecular Studies, 11350 SW Village  
Parkway, Port St. Lucie, FL 34987, USA  
e-mail: jmedina@tpims.org

D. Kuck · F. Lyko  
Division of Epigenetics, DKFZ-ZMBH Alliance, Deutsches  
Krebsforschungszentrum, Im Neuenheimer Feld 580, 69120  
Heidelberg, Germany

## Introduction

DNA methylation is an epigenetic change that results in the addition of a methyl group at the carbon-5 position of cytosine residues. The process is mediated by the DNA methyltransferase (DNMT) enzymes. To date, three DNMTs have been identified in the human genome, including the two novo methyltransferases (DNMT3a and DNMT3b) and the maintenance methyltransferase (DNMT1), which is the most abundant among the three [1]. DNMT1 is responsible for duplicating the pattern of DNA methylation during

replication and is essential for mammalian development. These enzymes are key regulators of gene transcription and their roles in carcinogenesis have been a topic of considerable interest over the last few years [2]. Therefore, specific inhibition of DNA methylation is an attractive and novel approach for cancer therapy [3,4].

The mechanism of DNA cytosine-C5 methylation is schematically depicted in Fig. 1 [5–8]. The thiol of the catalytic cysteine in the active site of DNMTs acts as a nucleophile that attacks the 6-position of the target cytosine to generate a covalent intermediate between the enzyme and DNA (Fig. 1, the residue numbers used throughout this study are based

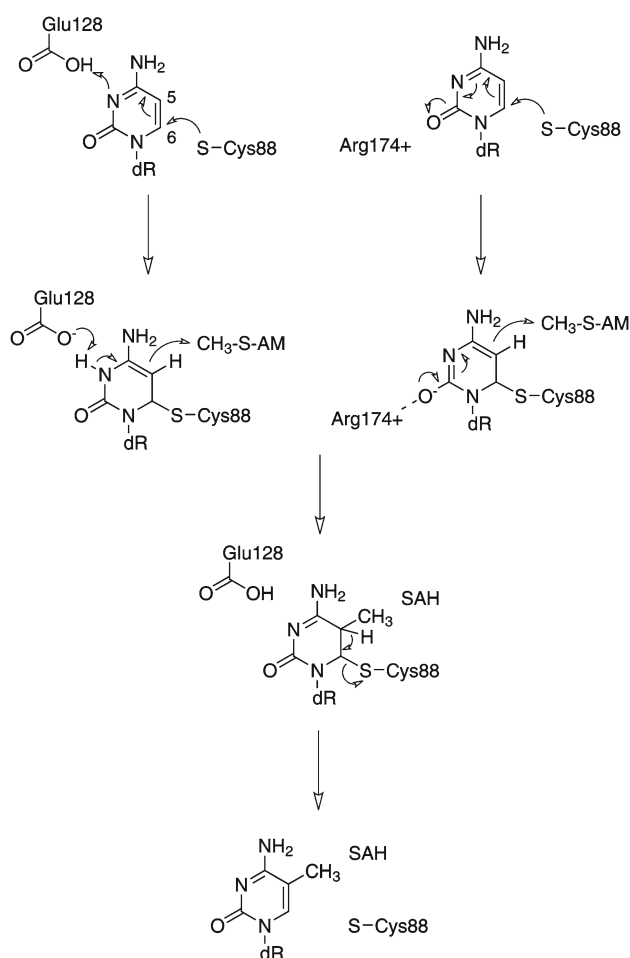


**Fig. 1** Mechanism of DNA methylation. The thiol of the catalytic cysteine attacks the 6-position of the target cytosine to generate a covalent intermediate. The 5-position of the cytosine is activated and attacks the methyl group of *S*-adenosyl-L-methionine (SAM) to form the 5-methyl covalent adduct and *S*-adenosyl-L-homocysteine (SAH). The attack on the 6-position is assisted by a transient protonation of the cytosine ring at the endocyclic nitrogen atom N3, which is stabilized by a glutamate residue (Glu128). The carbanion may also be stabilized by resonance where an arginine residue (Arg174) may play an important role. The covalent complex between the methylated base and the DNA is resolved by deprotonation at the 5-position to generate the methylated cytosine and the free enzyme

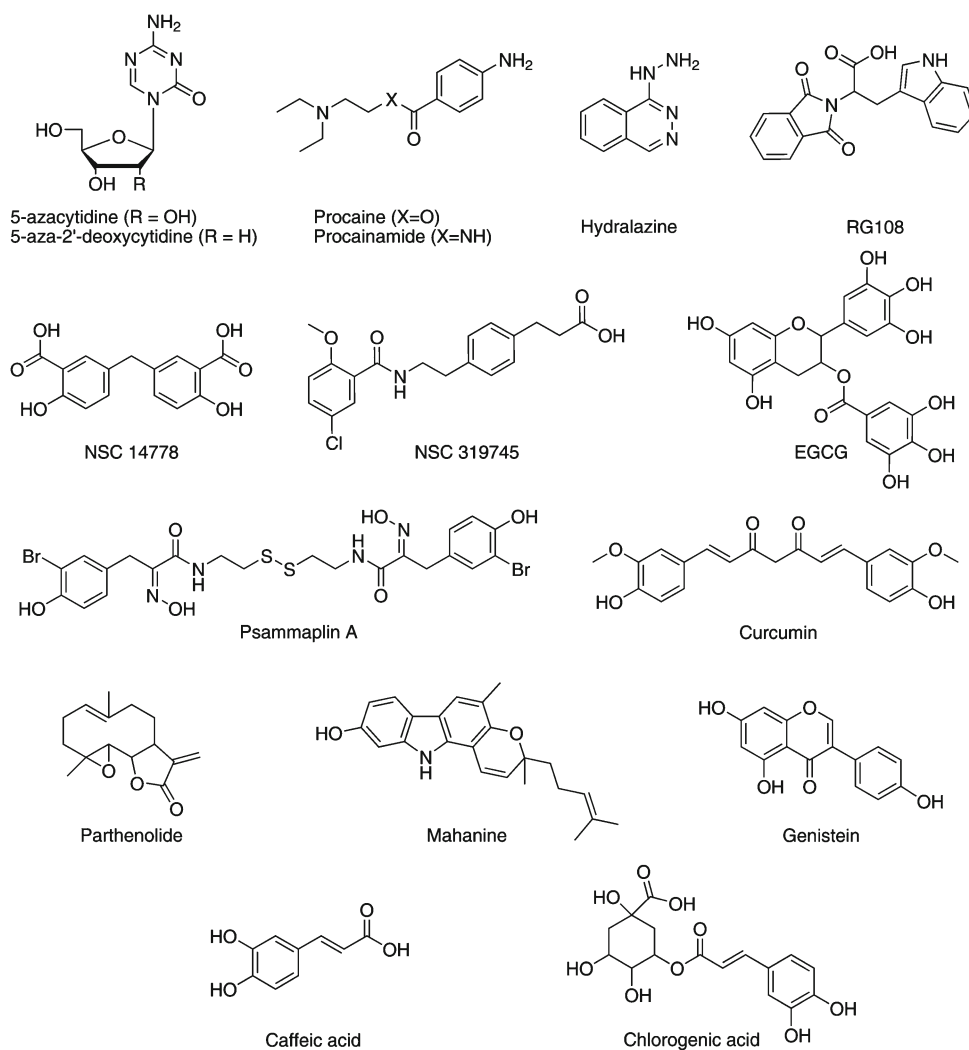
on the sequence numbers shown in Fig. S1 of Supplemental material).

The 5-position of the cytosine is activated and conducts a nucleophilic attack on the methyl group of the methyl-donating cofactor *S*-adenosyl-L-methionine (SAM) to form the 5-methyl covalent adduct and *S*-adenosyl-L-homocysteine (SAH). The attack on the 6-position is assisted by a transient protonation of the cytosine ring at the endocyclic nitrogen atom N3, which is stabilized by a glutamate residue (Glu128/Glu1266). The carbanion may also be stabilized by resonance [9] where an arginine residue (Arg174/Arg1312) may play an important role in the catalytic mechanism [10]. The covalent complex between the methylated base and the DNA is resolved by deprotonation at the 5-position to generate the methylated cytosine and the free enzyme [11].

Among the several known candidate DNMT inhibitors, only 5-azacytidine and 5-aza-2'-deoxycytidine (decitabine) (Fig. 2) have been developed clinically. These two drugs are nucleoside analogs, which, after incorporation into DNA, cause covalent trapping and subsequent depletion of DNMTs [12–14]. The mode of action of azanucleosides probably involves several additional cellular pathways. In addition, the specificity of azanucleosides is relatively low [13]. Consequently, these drugs are characterized by substantial cellular and clinical toxicity, which has driven the development of novel and more specific drugs. There is now an increasing number of substances that are reported to inhibit DNMTs [3]. Selected DNMT inhibitors and other candidate demethylating agents are depicted in Fig. 2. Some of these compounds are approved drugs for other indications (i.e., the antihypertensive drug hydralazine [15,16], the local anesthetic procaine [17], and the antiarrhythmic drug procainamide [18,19]). Others like the L-tryptophan derivative RG108, NSC 14778, and NSC 319745 (Fig. 2) have been identified by docking-based virtual screening [20,21].

The significant contributions of natural products in drug discovery [22–27] and anticancer drug development are well known [28–30]. For example, it is estimated that over 60% of the current anticancer drugs are directly or indirectly derived from natural sources [28]. Because environmental exposures are commonly assumed to play a major role in the establishment of abnormal DNA methylation patterns a constant uptake of DNA demethylating agents is believed to have a chemopreventive effect. This could be most conveniently achieved through the dietary uptake of natural product DNMT inhibitors [11,31,32]. A prominent example for this hypothesis is the main polyphenol compound from green tea, (–)-epigallocatechin-3-gallate (EGCG), which has been proposed to inhibit DNMT1 by blocking the active site of the enzyme and to reactivate methylation-silenced genes in cancer cells [33,34]. Other tea polyphenols such as catechin and epicatechin, and the bioflavonoids quercetin, fisetin and myricetin have also been implied in DNA

**Fig. 2** Chemical structures of selected DNMT inhibitors and other proposed demethylating agents



methylation inhibition. The catechol containing dietary epicatechin has been suggested to indirectly inhibit DNA methylation due to the increased formation of SAH, as a consequence of catechol-*O*-methyltransferase (COMT)-mediated *O*-methylation of epicatechin [34]. Other dietary catechols that may inhibit DNA methylation by a similar mechanism are the polyphenols from coffee, caffeic acid, and chlorogenic acid (Fig. 2) [35]. Apples polyphenols [36], the major isoflavone from soy bean genistein, and two other isoflavones, biochanin A and daidzein [37], have also been reported with demethylating activity (Fig. 2). Mahanine, a plant derived carbazole alkaloid (Fig. 2), has been reported to induce the ras-association domain family1 (RASSF1) gene in human prostate cancer cells, presumably by inhibiting DNMT activity [38]. Psammaplin A and several other disulfide bromotyrosine derivatives isolated from the marine sponge *Pseudoceratina purpurea* have been described as potent inhibitors of DNMT1 (Fig. 2) [39]. Other marine natural products with reported DNMT1 inhibitory activity are

the peyssonenyne A and B isolated from the red alga *Peyssonnelia caulifera* [40]. Lastly, curcumin, the major component of the Indian curry spice turmeric, and parthenolide, the principal sesquiterpene lactone of feverfew, have also been reported to inhibit DNMT1. Curcumin and parthenolide may act as mechanistic inhibitors, presumably by alkylating the catalytic cysteine of the DNMT1 binding site [41,42]. While the substantial number of recent reports may suggest that many natural products inhibit DNA methylation, it should be noted that only few reports provide compelling evidence for DNMT inhibition in biochemical and in cellular assays. As such, it remains possible that many of these compounds have an indirect and fortuitous effect on DNA methylation, but do not show a pharmacologically relevant activity that can be developed further for therapeutic purposes.

Molecular modeling has helped to understand the mechanism of established DNMT inhibitors at the molecular level. For example, molecular docking and dynamics studies of hydralazine have been used to characterize the interactions

of this molecule with the DNMT1 active site [43]. Docking models of EGCG with the catalytic site of DNMT1 have been proposed to substantiate the claim that EGCG blocks the active site of DNMT1 [33,34]. In addition, binding models with DNMT1 have been developed for parthenolide [42], curcumin and related compounds [41], to support the hypothesis that these natural products may alkylate the catalytic cysteine and covalently block the catalytic site. Lastly, the potential presence of DNMT inhibitors in dietary products and commonly used herbal remedies supports the identification of additional inhibitors of natural origin. The systematic search for active compounds in natural products databases can thus be the basis to further support the use of complementary and alternative medicine products for DNA methylation inhibition.

In this work, we reevaluate the activity of the two most prominent natural products associated with DNA methylation inhibition, EGCG and curcumin, and use computational techniques to identify novel potential DNMT inhibitors in a molecular database with more than 89,000 natural products. To the best of our knowledge, this is the first report towards a systematic screening of a diverse natural product collection for DNMT inhibitors. A selected subset of lead-like compounds was subjected to a multistep docking-based virtual approach. Since no crystallographic structure is available for the catalytic domain of DNMT1, the virtual screening was conducted using three docking programs with a previously validated homology model of the catalytic domain of human DNMT1 [44]. Compounds with promising DNMT1 binding characteristics and diverse chemical scaffolds were identified.

## Materials and methods

### Experimental evaluation of EGCG and curcumin

Biochemical DNMT1 assays were carried out as described previously [19]. Restriction enzyme digests with *Hha*I (New England Biolabs) were performed according to the manufacturer's protocol. 10 U of restriction enzyme was preincubated with EGCG at final concentrations of 10  $\mu$ M, 1  $\mu$ M, 100 nM, 10 nM, or 1 nM for 1 h at room temperature. Subsequently, a DNA substrate was added and the restriction digest was incubated for 1 h at 37°C, followed by analysis on a 2% Tris–borate EDTA agarose gel. The DNA substrate (400 ng) for the assay was a 798 bp fragment from the promoter region of the human *p16<sup>Ink4a</sup>* gene [45]. Genomic cytosine methylation levels of cells incubated for 72 h with EGCG and 5-azacytidine were determined by capillary electrophoretic analysis, as described previously [46].

### Natural product database preparation

A collection of natural products with 89,425 compounds was obtained from the ZINC database [47]. At the time of

download, the natural products available at ZINC contained compounds from seven vendors that advertise their compounds as being natural products or natural product derivatives. All entries in the collection contained one molecule (e.g., we did not detect salts). The same collection of natural products has been subject of a chemoinformatic analysis in our group (see below). A total of 89,037 molecules with unique SMILES were selected. In order to further select a subset of lead-like compounds the compound database was processed with the program Filter (version 2.0.2) [48]. Default parameters in the lead-like filter without further modifications were used. These parameters can be classified into three major categories, namely, molecular properties (molecular weight, topological polar surface area, log P, and aqueous solubility); atomic and functional group content (e.g., absolute and relative content of heteroatoms and limits on the number of several functional groups), and molecular graph topology (number and size of ring systems, flexibility of the molecule, and size and shape of non-ring chains). A complete list of the parameters used is presented in Table S1 of Supplemental material. The output lead-like natural products subset contained 14,053 unique compounds. Before docking, different protonation states (target pH  $7.0 \pm 2.0$ ) and tautomers were generated with Ligprep (version 2.2) [49]. Specified chiralities were retained and if the chirality is not specified, the two possible chiralities were generated. Preparation of the database with LigPrep yielded 19,873 structures.

### Scaffold and chemical space analysis of the lead-like natural products

The molecular scaffold content of the 14,053 unique compounds in the lead-like subset was analyzed. In this work, the scaffolds were defined as the *cyclic systems* that result from iteratively removing all vertices of degree one, in other words, by iteratively removing the side chains of the molecule. The cyclic systems are part of the chemotype methodology developed by Xu and Johnson [50,51], and were calculated with the program Molecular Equivalent Indices. The cyclic systems are similar to the *topological scaffolds* of Xu [52,53] or the *atomic frameworks* of Bemis and Murcko [54]. In the methodology used here, a chemotype code or chemotype identifier (a code of five characters), is assigned to each cyclic system using a unique naming algorithm [50]. Although different *resolution levels* are possible in scaffold analysis, for example, by assigning one single atom and bond type (e.g., *cyclic system skeletons* in the chemotype methodology of Xu and Johnson [51]) we focus this study on cyclic systems. This methodology has been recently applied in our group to analyze the scaffold content of natural products and other compound databases [55–58].

A visual representation of the chemical space [56] of the lead-like natural products was generated by principal

component analysis of six scaled molecular properties computed with the program Molecular Operating Environment (MOE) (version 2008.10) [59], namely molecular weight (MW), number of hydrogen bond donors (HBD), number of hydrogen bond acceptors (HBA), number of rotatable bonds (RB), SlogP, and topological polar surface area (TPSA). The chemical or property space of other compound databases has been compared by our group using the same molecular properties [57].

#### Docking-based virtual screening

The general multistep docking approach implemented in this work is described ahead and it is based on a previous successful virtual screening of the NCI database [21] (see also Fig. 5a). The natural products lead-like set previously prepared with Ligprep, as described above, was docked with a validated homology model of the catalytic domain of human DNMT1 using Glide (version 5.0) [60]. The coordinates of the homology model published previously were the starting point [44]. We employed the same scoring grids and docking parameters of Glide Standard Precision (SP) reported for the virtual screening of the NCI database with DNMT1 [21]. The 2,000 top scoring molecules (Glide SP score  $< -6.58$ ) were independently docked with Glide Extra Precision (XP) and Gold (version 4.1) [61]. In Gold, the binding site was defined by selecting all atoms within 10 Å of 2'-deoxycytidine (as found in the binding model we reported previously [43]) with the cavity detection mode turned on. A maximum of 50 docking runs per molecule were performed allowing early termination if top three solutions are within 1.5 Å RMS deviations of each other. The number of genetic operations was set to 100,000. Poses were evaluated with GoldScore. Cys88 was allowed to rotate freely during docking [20]. A total of 64 consensus compounds with unique SMILES and Glide XP score  $\leq -7.0$  (488 compounds) and GoldScore  $\geq 62.0$  (271 compounds) were selected. These cutoff values were based on the docking scores of RG108 that was taken as a reference (compounds with similar or better docking scores than RG108 were selected). The 64 Glide XP-Gold consensus compounds were further docked with Autodock (version 4.0) [62,63]. AutoDock tools (ADT) (version 1.4.5) were used for protein and ligand preparation. Briefly, all hydrogen, including non-polar, Kollman charges, and solvation parameters were added. After adding charges, the non-polar hydrogens were merged. The auxiliary program Autogrid was used to generate the grid maps; where each map was centered at the coordinates of docked 2'-deoxycytidine with the model of DNMT1 as recently reported by our group [21]. The grid dimensions were set to  $60 \times 40 \times 40$ , adjusting the spacing between the grid points to 0.375 Å. For all ligands, Gasteiger charges [64] were assigned and then non-polar hydrogens were merged. All bond rotations for ligands

were automatically set in ADT and the Lamarckian genetic algorithm (LGA) was employed. The number of the docking runs was set to 10 and the solutions for each docked ligand were clustered into groups with RMSDs  $< 1.0$  Å.

Among the 64 GlideXP-Gold consensus hits, a total of 58 compounds with Autodock Energy  $\leq -8.61$  (taking RG108 as reference) were identified. This set can be regarded as *GlideXP-Gold-Autodock consensus hits*. In order to explore the putative interactions of the virtual screening hits with DNMT1, the ligand-protein complexes obtained with docking were subjected to full energy minimization using the MMFF94x force field implemented in MOE until the gradient 0.001 was reached. The default parameters implemented into the MOE's LigX application were used [59].

#### Molecular properties profiling

Selected properties were computed for the consensus virtual screening hits with MOE (version 2008.10) [59].

## Results and discussion

#### Experimental reevaluation of EGCG and curcumin

The potential demethylating activity of the green tea polyphenol EGCG is being discussed controversially. The experimental evidence supporting DNA demethylation in human cancer cells is limited to indirect PCR analyses of a few cancer-associated genes [33] and could not be reproduced by more comprehensive and direct experimental approaches [65,66]. In addition, it was noted that EGCG is a highly reactive compound that might thus inhibit DNA methylation non-specifically and/or indirectly [66]. To directly evaluate the inhibitory activity of EGCG, we tested the compound in a biochemical assay with purified human DNMT1. The results showed a detectable inhibition of methyltransferase activity, with an  $IC_{50}$  concentration of 70  $\mu$ M (Fig. 3a). In a control experiment, we subsequently tested EGCG in a completely different reaction and determined the ability of the compound to inhibit the restriction enzyme *HhaI*. The results showed readily detectable inhibition of the restriction enzyme in a concentration range from 10  $\mu$ M to 1 nM (Fig. 3b). These findings suggest that enzyme inhibition is caused by the chemical reactivity of EGCG and further support the notion that EGCG should not be considered as a DNMT inhibitor.

In subsequent experiments, we also evaluated the DNA demethylating activity of curcumin, the major component of the Indian spice turmeric, which has been shown to affect multiple biological pathways, including DNA methylation [41]. However, the conclusion that curcumin is a hypomethylating agent was based on the analysis of DNA from a single



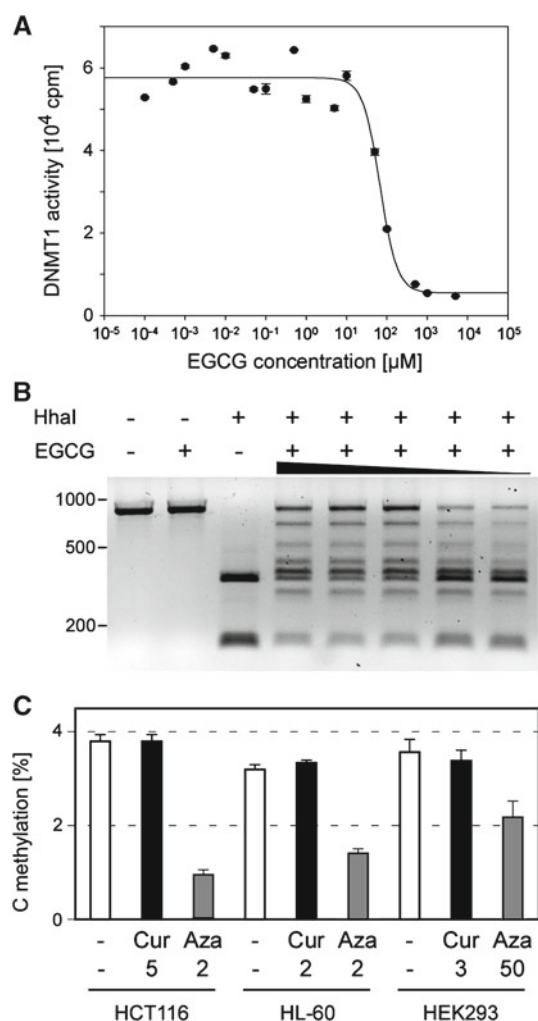


**Fig. 3** Experimental evaluation of EGCG and curcumin as potential demethylating drugs. **a** Dose–response plots of EGCG against purified recombinant DNMT1. Each data point represents the mean  $\pm$  SD of three measurements and an  $\text{IC}_{50}$  concentration of  $70 \mu\text{M}$  was determined from the data. **b** Inhibition of the *HhaI* restriction enzyme by EGCG. Purified recombinant *HhaI* was treated with EGCG (concentration range  $10 \mu\text{M}$ – $1 \text{nM}$ ) and then used in a restriction assay with a 800 bp DNA fragment. **c** Curcumin does not cause DNA demethylation in three arbitrarily chosen human cancer cell lines. Cells were incubated for 72 h with the drug-specific  $\text{IC}_{50}$  concentration of curcumin (Cur) or 5-azacytidine (Aza), as indicated (in  $\mu\text{M}$ ). Cytosine methylation levels were determined by capillary electrophoretic analysis of genomic DNA from drug-treated cells

curcumin-treated leukemia cell line that revealed a comparably small (15–20%) decrease in methylation at micromolar drug concentrations. We therefore evaluated the effect of curcumin to induce DNA hypomethylation in three independent human cancer cell lines. Using conditions highly similar to those reported previously [41], we could not detect any curcumin-dependent demethylation (Fig. 3c). In contrast, 5-azacytidine induced robust demethylation in all three cell lines (Fig. 3c). These results, together with the low specificity of

the compound [41], suggest that curcumin has little or no pharmacologically relevant activity as a DNMT inhibitor.

#### Lead-like natural products database: selection and chemoinformatic analysis

To identify novel candidate DNMT inhibitors of natural origin we used virtual screening. The natural products collection, as implemented in the ZINC database [47], is a public compilation of commercially available compounds. The natural product database used for this study contained 89,425 molecules. Recently, the same data set was subject of a chemoinformatic analysis in our group establishing the most frequent molecular scaffolds and comparing the chemical space coverage with a collection of approved drugs [67]. In this work, in order to focus the virtual screening on compounds that could be promising for further development as DNMT1 inhibitors, we selected a subset of lead-like natural products [68]. The selection was made based on properties and functional groups using the Filter program [48] reducing the initial database to a subset of 14,053 lead-like natural products.

The lead-like natural products subset was analyzed in terms of molecular scaffolds as described in the “Materials and methods” section. We found that in the subset with 14,053 lead-like compounds there are 3,144 (22.4%) different molecular scaffolds. A total of 1,398 (9.9%) scaffolds are singletons (i.e., scaffolds with only one molecule). Comparing these values with the proportions reported for the entire natural product collection (17.9% scaffolds and 7.2% singletons) [57], suggests a larger degree of scaffold diversity in the lead-like subset. Figure 4a depicts the most frequent molecular scaffolds in the lead-like natural product set along with the corresponding chemotype identifier. Scaffolds with a frequency of at least 98 are shown. Other than benzene, which is a very common scaffold found in drugs and other compound collections [54,57,58], the most frequent scaffold in the lead-like set is the benzopyran-2-one (chromen-2-one or coumarin) (frequency of 710, 5.05%), followed by indole (224, 1.59%), 2-phenyl-4*H*-chromen-4-one (205, 1.46%), and 2-phenyl-1,4-benzopyrone or flavone (205, 1.46%). These scaffolds along with others marked in bold in Fig. 4a are also frequent in the initial non-filtered natural product collection [57].

Figure 4b depicts a three-dimensional representation of the chemical space [56] of the lead-like subset as defined by six molecular properties namely MW, HBD, HBA, RB, SlogP, and TPSA (see “Materials and methods” section). The chemical or property space was compared to a collection of 1,490 drugs obtained from DrugBank [67]. The first three principal components with eigenvalues 2.55, 1.38, and 0.94, respectively, account for 81% of the variance and are depicted in Fig. 4b. The first principal component is associated mainly

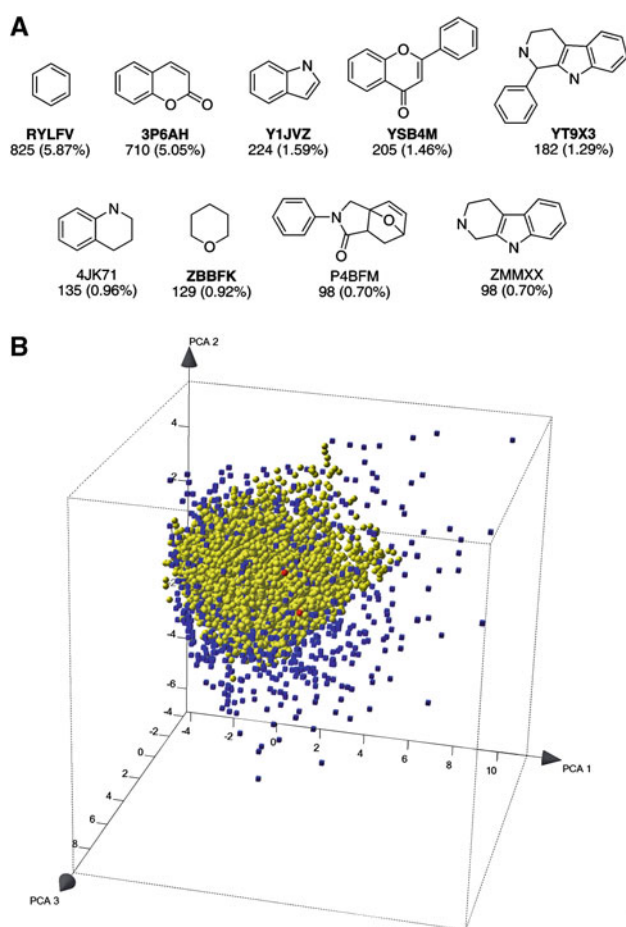


**Fig. 4** Chemoinformatic analysis of 14,053 compounds in the lead-like set of natural products. **a** Most frequent molecular scaffolds (cyclic systems). Chemotype identifier, frequency and percentage are shown. The chemotype identifier of scaffolds also frequent in the non-filtered natural product database [57] is in *bold*. **b** Three-dimensional representation of the property space of the lead-like set of natural products (*yellow spheres*) and a collection of 1,490 drugs (*blue squares*). The visual representation of the property space was obtained by principal component analysis of six scaled molecular properties (MW, RB, HBA, HBD, TPSA, and SlogP). The first three principal components account for 81% of the variance. The first principal component is associated mainly with TPSA; the second principal component is mostly related to SlogP whereas the third principal component is mainly associated with RB and HBD (Table S2 of Supplemental material summarizes the corresponding loadings and eigenvalues for the first three principal components). Representative virtual screening hits (Fig. 5) are marked in *red*. A two-dimensional representation of the property space is depicted in Fig. S2 of Supplemental material. (Color figure online)

with TPSA; the second principal component is mostly related to SlogP whereas the third principal component is mainly associated with RB and HBD (Table S2 of Supplemental material summarizes the corresponding loadings and eigenvalues for the first three principal components). This analysis clearly supported the fact that the lead-like natural products subset is contained within the biologically relevant property space covered by drugs and it is an attractive set to

conduct virtual screening. A two-dimensional representation of the chemical space is shown in Fig. S2 of Supplemental material.

#### Docking-based virtual screening

The lead-like natural products set was docked with the catalytic site of human DNMT1 using a multistep docking approach (Fig. 5a). The homology model used in this work has been successfully used for previous virtual screening [20,21] and modeling studies [43] (the amino acid sequence of the homology model of DNMT1 used in this study is shown in Fig. S1 of Supplemental material). Multistep or cascade docking is a general virtual screening strategy recently reviewed in [69] that has been successful to identify novel DNMT inhibitors [20,21]. In this work, the lead-like set was further filtered with Glide SP selecting the 2,000 top-ranked poses. These poses were further docked with Glide XP and Gold. Consensus hits were selected as described in “Materials and methods” section and docked with Autodock4. A total of 58 consensus hits, with favorable docking scores by all three docking programs, Glide XP, Gold and Autodock, were identified (Fig. 5a). Similar to the criterion applied in the virtual screening of the NCI database with DNMT1 [21], consensus hits were selected based on the corresponding docking scores of the prototypical DNMT inhibitor RG108 that was used as a reference (see “Materials and methods” section). Consensus hits showed similar or more favorable docking scores than RG108 by all three docking programs. The chemical structures of *representative* consensus hits by all three docking programs are presented in Fig. 5b (additional consensus hits are shown in Fig S3 of Supplemental material). The docking scores and selected properties are presented in Table 1.

Interestingly, the methylenedisalicylic acid derivative, ZINC04028795 (Fig. 5b), was also identified as a hit in the virtual screening of the NCI database, which we recently reported [21]. This compound (also known as NCI 408488) reduced the enzymatic activity of DNMT1 by 22% at 100  $\mu$ M compound concentration against 800 nM of DNMT1 [21]. Noteworthy, ZINC04028795 was 5% more active than RG108 under the same experimental conditions (i.e., the relative enzymatic activity was as follows:  $78 \pm 3.8\%$  inhibition for ZINC04028795 as compared to  $83 \pm 3.2\%$  inhibition for RG108) [21].

Several consensus hits of the virtual screening of the lead-like natural products have a coumarin scaffold (Fig. 4a). Examples are compounds ZINC00082754, 00488951, 00519227, 02115624, and 02122993 (Fig. 5b). Another compound with a coumarin ring is ZINC00319084. The high frequency of occurrence can be related to the relatively high frequency of the coumarin scaffold in the initial set of the screened compounds as revealed by the chemoinformatic

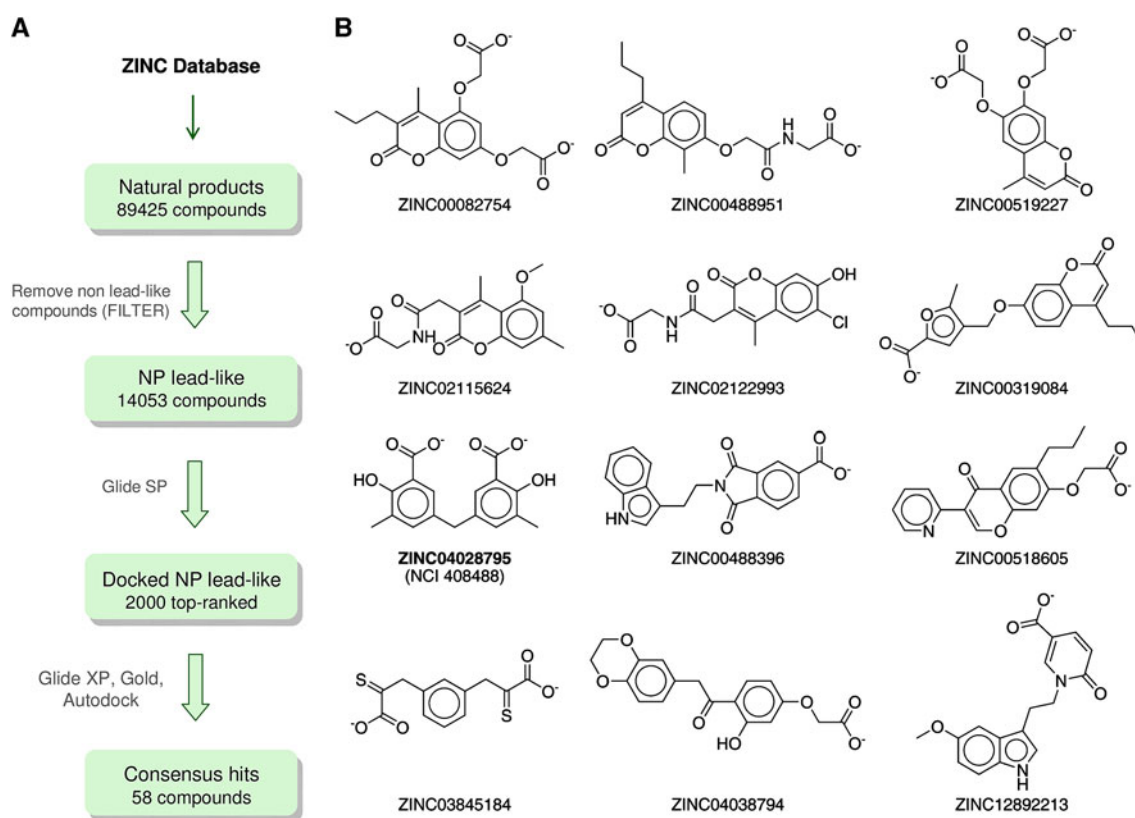


**Fig. 5** Discovery of novel candidate DNMT1 inhibitors by multi-step docking-based virtual screening approach. **a** Schematic outline of the screening cascade used in this work. **b** Chemical structures of 12

selected consensus hits with potential DNMT1 inhibitory activity. The chemical structures of the remaining 46 hits are shown in Fig. S3 of Supplemental material

**Table 1** Calculated lead-like and ADMET related properties and docking scores of *representative* virtual screening hits. The docking scores of the reference compound, RG108 are also included

Compound (ZINC ID)	MW	SlogP	logS	RB	HBA	HBD	TPSA	Autodock4 docking energy	Goldscore Fitness	Glide XP
00082754	350.3	2.1	−4.2	8	7	4	119.4	−11.43	69.34	−9.98
00319084	342.3	4.2	−6.0	6	4	2	86.0	−10.50	76.53	−7.30
00488396	334.3	2.7	−4.0	4	4	3	90.5	−12.05	68.82	−8.62
00488951	333.3	1.7	−4.5	8	5	3	101.9	−12.05	71.13	−8.75
00518605	339.3	3.1	−4.4	6	5	2	85.7	−11.31	67.45	−8.38
00519227	308.2	0.9	−3.2	6	7	4	119.4	−11.09	64.97	−9.88
02115624	319.3	1.3	−3.7	6	5	3	101.9	−11.55	62.38	−8.75
02122993	325.7	1.3	−3.5	5	5	4	112.9	−10.64	65.21	−8.73
03845184	286.4	1.5	−3.4	6	4	4	152.2	−10.16	68.21	−9.08
04028795	316.3	2.7	−3.0	4	6	6	115.1	−10.89	62.34	−9.72
04038794	344.3	2.1	−3.5	6	7	3	102.3	−10.5	69.76	−10.20
12892213	312.3	2.1	−2.8	5	4	3	82.6	−11.14	62.41	−9.23
RG108 (reference)	334.3	2.5	−4.0	4	4	3	90.5	−8.96	65.43	−5.99

Properties calculated with MOE. *logS* Log of aqueous solubility (mol/L), *RB* rotatable bonds, *HBA*, *HBD* hydrogen bond acceptors and donors, respectively. Autodock docking energy and Glide XP scores are in kcal/mol. GoldScore Fitness is the negative of the sum of the component energy terms employed in the scoring function



analysis described above (Fig. 4a). Interestingly, coumarin derivatives have diverse biological activities and have found multiple therapeutic applications, including antitumor activity [70,71]. The specific role of coumarin derivatives in breast cancer therapy has been reviewed recently [70]. Hits with other distinct molecular scaffolds were also obtained, such as the methylenedisalicylic acid derivative ZINC04028795 (see above), and molecules ZINC00488396, 00518605, 003845184, 04038794, and 12892213 (Fig. 5b). Of note, ZINC00488396 is structurally similar to RG108.

A notable feature of the consensus hits is the presence of a carboxylic acid group in the side chains (Fig. 5b). This feature was also present in the structure of the consensus hits of the virtual screening of the NCI database [21]. In these compounds, the carboxylic acid group can potentially have key interactions with the side chains of arginine residues present in the binding site such as Arg174 and Arg318. This is illustrated in Fig. 6 that shows the optimized binding model of ZINC00082754 with DNMT1 obtained with Autodock4. According to this model, one of the carboxylic acid groups form hydrogen bonds with His321 and His322. The second carboxylic acid group of ZINC00082754 forms hydrogen bonds with the side chains of Arg174 and Arg318. Similar hydrogen bonds with Arg174 are also predicted for 2'-deoxycytidine, 5-aza-2'-deoxycytidine and other inhibitors [43] and could be pharmacophoric interactions.

#### Properties of virtual screening hits

Table 1 summarizes molecular properties calculated with MOE for the *representative* consensus hits in Fig. 5b [59] (see “Materials and methods” section). Of note, all the hits have a molecular profile compliant with the values expected for typical drugs [57]. Similarly, the calculated SlogP value is equal or lower than 4.2, which is compliant with the value observed in most marketed drugs. In a recent study of the molecular properties of 24 natural products that were the starting point for marketed drugs in the 25-year period 1981–2006, it was concluded that maintaining low hydrophobicity regardless of other characteristics is “the single most important lesson from natural products” [23]. The biological relevance of the consensus hits as candidate compounds for further development is also illustrated in Fig. 4 and Fig. S2 in Supplemental material. The virtual screening hits, marked in red in both figures, are contained within the drug-relevant property space. These findings are not sufficient to establish the compounds as viable drug candidates, but they further support the notion that our virtual screening hits are attractive compounds for development. If active against DNMTs, the virtual screening hits of natural origin should undergo the same iterative cycles of development as other hits and leads obtained from different sources [23].

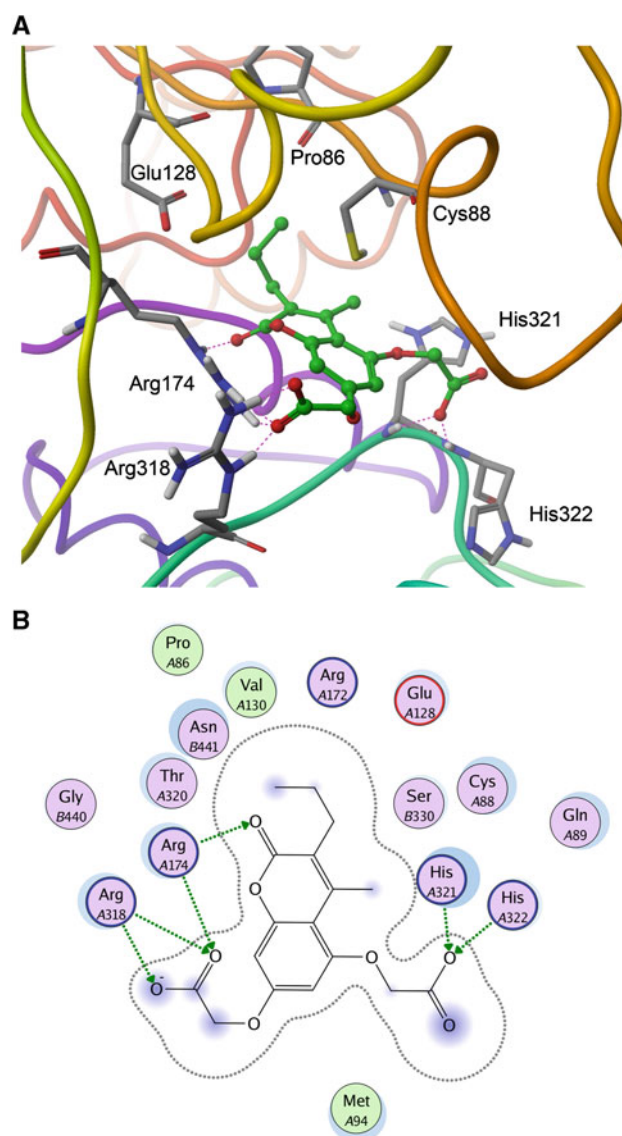


**Fig. 6** Optimized binding model of virtual screening hit ZINC 00082754 with human DNMT1. **a** Three-dimensional representation displaying selected amino acid residues. Hydrogen bonds are indicated with magenta dashes. **b** Two-dimensional interaction map displaying amino acid residues within 4.5 Å of the ligand. The ligand proximity contour is depicted with a dotted line. The ligand solvent exposure is represented with blue circles; larger and darker circles on ligand atoms indicate more solvent exposure. The receptor solvent exposure differences—in the presence and absence of the ligand—are represented by the size and intensity of the turquoise discs surrounding the residues; larger and darker discs indicate residues highly exposed to solvent in the active site when the ligand is absent. Figure created with the Ligand Interactions application of MOE [59]. (Color figure online)

#### Conclusions and perspectives

We report a systematic computational screening of a large collection of natural products as DNMT1 inhibitors. To the best of our knowledge, this is the first *in silico* study of a large database of natural products towards the identification of novel com-

pounds with inhibitory activity of DNMTs. Starting with a publicly available database containing more than 89,000 compounds, we selected a lead-like subset with approximately 14,000 molecules. Comparison of the property space of the lead-like subset with a collection of approved drugs further confirmed the drug-related biological relevance of the natural products subset. In addition, a scaffold analysis of the lead-like subset revealed that, other than benzene, the most frequent scaffolds in this set are benzopyran-2-one (chromen-2-one or coumarin), indole, and 2-phenyl-1,4-benzopyrone or flavone. Virtual screening of the lead-like natural product set with a validated homology model of the catalytic domain of DNMT1 was conducted following a multistep docking-based approach using Glide, Gold, and Autodock. A total of 58 consensus hits with high and similar or better docking scores than the corresponding scores for RG108 were identified. The consensus hit ZINC04028795 or NCI 408488 has reported DNMT1 inhibitory activity [21]. Another hit, compound ZINC00488396, is a structural isomer of RG108. The consensus hits are characterized by side chains containing carboxylic groups which permit hydrogen bonds with amino residues that have an important role in the mechanism of DNA methylation. The molecular properties of the virtual screening hits are compliant with the biological relevant property space covered by drugs.

A major perspective of this work is the experimental validation of the consensus hits. In addition, the multistep docking-based strategy used in this work can be implemented to screen other larger in-house or commercial natural products databases such as the CRC Dictionary of Natural Products [72] or the database implemented in the Drug Discovery Portal [73]. On a more general level, our results also reinforce the notion that compounds with DNA demethylating activity can be found in natural sources, including dietary products. While we were unable to determine the sources of the hits identified in this study, our results suggest that natural products are a rich source for demethylating agents that need to be rigorously characterized in biochemical and cellular assays.

**Acknowledgements** This work was supported by the State of Florida, Executive Office of the Governor's Office of Tourism, Trade, and Economic Development. J.L.M.-F. wishes to thank the Menopause & Women's Health Research Center for support. The authors are grateful to OpenEye Scientific Software, Inc. for providing the FILTER program.

## References

- Goll MG, Bestor TH (2005) Eukaryotic cytosine methyltransferases. *Annu Rev Biochem* 74:481–514. doi:10.1146/annurev.biochem.74.010904.153721
- Jones PA, Baylin SB (2007) The epigenomics of cancer. *Cell* 128:683–692. doi:10.1016/j.cell.2007.01.029
- Lyko F, Brown R (2005) DNA methyltransferase inhibitors and the development of epigenetic cancer therapies. *J Natl Cancer Inst* 97:1498–1506. doi:10.1093/jnci/dji311
- Brueckner B, Kuck D, Lyko F (2007) DNA methyltransferase inhibitors for cancer therapy. *Cancer J* 13:17–22. doi:10.1097/PPO.0b013e31803c7245
- Santi DV, Garrett CE, Barr PJ (1983) On the mechanism of inhibition of DNA cytosine methyltransferases by cytosine analogs. *Cell* 33:9–10. doi:10.1016/0092-8674(83)90327-6
- Wu JC, Santi DV (1987) Kinetic and catalytic mechanism of *HhaI* methyltransferase. *J Biol Chem* 262:4778–4786
- Chen L, Macmillan AM, Chang W, Ezaznikpay K, Lane WS, Verdine GL (1991) Direct identification of the active-site nucleophile in a DNA (cytosine-5)-methyltransferase. *Biochemistry* 30:11018–11025. doi:10.1021/bi00110a002
- Ogara M, Klimasauskas S, Roberts RJ, Cheng XD (1996) Enzymatic C5-cytosine methylation of DNA: mechanistic implications of new crystal structures for *HhaI* methyltransferase-DNA-AdoHcy complexes. *J Mol Biol* 261:634–645. doi:10.1006/jmbi.1996.0489
- Kumar S, Horton JR, Jones GD, Walker RT, Roberts RJ, Cheng X (1997) DNA containing 4'-thio-2'-deoxycytidine inhibits methylation by *HhaI* methyltransferase. *Nucleic Acids Res* 25:2773–2783. doi:10.1093/nar/25.14.2773
- Jurkowski TP, Meusburger M, Phalke S, Helm M, Nellen W, Reuter G, Jeltsch A (2008) Human DNMT2 methylates tRNA(Asp) molecules using a DNA methyltransferase-like catalytic mechanism. *RNA* 14:1663–1670. doi:10.1261/rna.970408
- Suzuki T, Miyata N (2006) Epigenetic control using natural products and synthetic molecules. *Curr Med Chem* 13:935–958. doi:10.2174/092986706776361067
- Liu K, Wang YF, Cantemir C, Muller MT (2003) Endogenous assays of DNA methyltransferases: evidence for differential activities of DNMT1, DNMT2, and DNMT3 in mammalian cells in vivo. *Mol Cell Biol* 23:2709–2719. doi:10.1128/mcb.23.8.2709-2719.2003
- Stresemann C, Lyko F (2008) Modes of action of the DNA methyltransferase inhibitors azacytidine and decitabine. *Int J Cancer* 123:8–13. doi:10.1002/ijc.23607
- Schermelleh L, Spada F, Easwaran HP, Zolghadr K, Margot JB, Cardoso MC, Leonhardt H (2005) Trapped in action: direct visualization of DNA methyltransferase activity in living cells. *Nat Methods* 2:751–756. doi:10.1038/nmeth794
- Segura-Pacheco B, Trejo-Becerril C, Perez-Cardenas E, Taja-Chayeb L, Mariscal I, Chavez A, Acuna C, Salazar AM, Lizano M, Duenas-Gonzalez A (2003) Reactivation of tumor suppressor genes by the cardiovascular drugs hydralazine and procainamide and their potential use in cancer therapy. *Clin Cancer Res* 9:1596–1603
- Segura-Pacheco B, Perez-Cardenas E, Taja-Chayeb L, Chavez-Blanco A, Revilla-Vazquez A, Benitez-Bribiesca L, Duenas-Gonzalez A (2006) Global DNA hypermethylation-associated cancer chemotherapy resistance and its reversion with the demethylating agent hydralazine. *J Transl Med* 4:32. doi:10.1186/1479-5876-4-32
- Villar-Garea A, Fraga MF, Espada J, Esteller M (2003) Procaine is a DNA-demethylating agent with growth-inhibitory effects in human cancer cells. *Cancer Res* 63:4984–4989
- Lee BH, Yegnasubramanian S, Lin XH, Nelson WG (2005) Procainamide is a specific inhibitor of DNA methyltransferase 1. *J Biol Chem* 280:40749–40756. doi:10.1074/jbc.M505593200
- Castellano S, Kuck D, Sala M, Novellino E, Lyko F, Sbardella G (2008) Constrained analogues of procaine as novel small molecule inhibitors of DNA methyltransferase-1. *J Med Chem* 51:2321–2325. doi:10.1021/jm7015705

20. Siedlecki P, Boy RG, Musch T, Brueckner B, Suhai S, Lyko F, Zielenkiewicz P (2006) Discovery of two novel, small-molecule inhibitors of DNA methylation. *J Med Chem* 49:678–683. doi:10.1021/jm050844z
21. Kuck D, Singh N, Lyko F, Medina-Franco JL (2010) Novel and selective DNA methyltransferase inhibitors: docking-based virtual screening and experimental evaluation. *Bioorg Med Chem* 18:822–829. doi:10.1016/j.bmc.2009.11.050
22. Harvey AL (2008) Natural products in drug discovery. *Drug Discov Today* 13:894–901. doi:10.1016/j.drudis.2008.07.004
23. Ganesan A (2008) The impact of natural products upon modern drug discovery. *Curr Opin Chem Biol* 12:306–317. doi:10.1016/j.cbpa.2008.03.016
24. Butler MS (2008) Natural products to drugs: natural product-derived compounds in clinical trials. *Nat Prod Rep* 25:475–516. doi:10.1039/b514294f
25. Newman DJ (2008) Natural products as leads to potential drugs: an old process or the new hope for drug discovery?. *J Med Chem* 51:2589–2599. doi:10.1021/jm0704090
26. Molinski TF, Dalisay DS, Lievens SL, Saludes JP (2009) Drug development from marine natural products. *Nat Rev Drug Discov* 8:69–85. doi:10.1038/nrd2487
27. Demain AL, Sanchez S (2009) Microbial drug discovery: 80 years of progress. *J Antibiot* 62:5–16. doi:10.1038/ja.2008.16
28. Cragg GM, Newman DJ (2009) Nature: a vital source of leads for anticancer drug development. *Phytochem Rev* 8:313–331. doi:10.1007/s11101-009-9123-y
29. Coseri S (2009) Natural products and their analogues as efficient anticancer drugs. *Mini-Rev Med Chem* 9: 560–571. doi:10.2174/138955709788167592
30. Kinghorn AD, Chin YW, Swanson SM (2009) Discovery of natural product anticancer agents from biodiverse organisms. *Curr Opin Drug Discov Dev* 12:189–196
31. Hauser AT, Jung M (2008) Targeting epigenetic mechanisms: potential of natural products in cancer chemoprevention. *Planta Med* 74:1593–1601. doi:10.1055/s-2008-1081347
32. Yu N, Wang M (2008) Anticancer drug discovery targeting DNA hypermethylation. *Curr Med Chem* 15:1350–1375. doi:10.2174/092986708784567653
33. Fang MZ, Wang YM, Ai N, Hou Z, Sun Y, Lu H, Welsh W, Yang CS (2003) Tea polyphenol (–)-epigallocatechin-3-gallate inhibits DNA methyltransferase and reactivates methylation-silenced genes in cancer cell lines. *Cancer Res* 63:7563–7570
34. Lee WJ, Shim JY, Zhu BT (2005) Mechanisms for the inhibition of DNA methyltransferases by tea catechins and bioflavonoids. *Mol Pharmacol* 68:1018–1030. doi:10.1124/mol.104.008367
35. Lee WJ, Zhu BT (2006) Inhibition of DNA methylation by caffeic acid and chlorogenic acid, two common catechol-containing coffee polyphenols. *Carcinogenesis* 27:269–277. doi:10.1093/carcin/bgi206
36. Fini L, Selgrad M, Fogliano V, Graziani G, Romano M, Hotchkiss E, Daoud YA, De Vol EB, Boland CR, Ricciardiello L (2007) Anurca apple polyphenols have potent demethylating activity and can reactivate silenced tumor suppressor genes in colorectal cancer cells. *J Nutr* 137: 2622–2628. doi:10.3945/jn.109.118521
37. Fang MZ, Chen DP, Sun Y, Jin Z, Christman JK, Yang CS (2005) Reversal of hypermethylation and reactivation of *p16<sup>INK4a</sup>*, *RAR $\beta$* , and *MGMT* genes by genistein and other isoflavones from soy. *Clin Cancer Res* 11:7033–7041. doi:10.1158/1078-0432.ccr-05-0406
38. Jagadeesh S, Sinha S, Pal BC, Bhattacharya S, Banerjee PP (2007) Mahanine reverses an epigenetically silenced tumor suppressor gene RASSF1A in human prostate cancer cells. *Biochem Biophys Res Commun* 362:212–217. doi:10.1016/j.bbrc.2007.08.005
39. Pina IC, Gautschi JT, Wang GYS, Sanders ML, Schmitz FJ, France D, Cornell-Kennon S, Sambucetti LC, Remiszewski SW, Perez LB, Bair KW, Crews P (2003) Psammaplins from the sponge *Pseudoceratina purpurea*: inhibition of both histone deacetylase and DNA methyltransferase. *J Org Chem* 68:3866–3873. doi:10.1021/jo034248t
40. McPhail KL, France D, Cornell-Kennon S, Gerwick WH (2004) Peyssonenynes A and B, novel enediynes with DNA methyl transferase inhibitory activity from the red marine alga *Peyssonnelia caulifera*. *J Nat Prod* 67:1010–1013. doi:10.1021/np0400252
41. Liu ZF, Liu SJ, Xie ZL, Pavlovicz RE, Wu J, Chen P, Aimiuwu J, Pang JX, Bhasin D, Neviani P, Fuchs JR, Plass C, Li PK, Li C, Huang THM, Wu LC, Rush L, Wang HY, Perrotti D, Marcucci G, Chan KK (2009) Modulation of DNA methylation by a sesquiterpene lactone parthenolide. *J Pharmacol Exp Ther* 329:505–514. doi:10.1124/jpet.108.147934
42. Liu ZF, Xie ZL, Jones W, Pavlovicz RE, Liu SJ, Yu JH, Li PK, Lin JY, Fuchs JR, Marcucci G, Li CL, Chan KK (2009) Curcumin is a potent DNA hypomethylation agent. *Bioorg Med Chem Lett* 19:706–709. doi:10.1016/j.bmcl.2008.12.041
43. Singh N, Dueñas-González A, Lyko F, Medina-Franco JL (2009) Molecular modeling and dynamics studies of hydralazine with human DNA methyltransferase 1. *ChemMedChem* 4:792–799. doi:10.1002/cmde.200900017
44. Siedlecki P, Boy RG, Comagic S, Schirmacher R, Wiessler M, Zielenkiewicz P, Suhai S, Lyko F (2003) Establishment and functional validation of a structural homology model for human DNA methyltransferase 1. *Biochem Biophys Res Commun* 306:558–563. doi:10.1016/s0006-291x(03)01000-3
45. Brueckner B, Boy RG, Siedlecki P, Musch T, Kliem HC, Zielenkiewicz P, Suhai S, Wiessler M, Lyko F (2005) Epigenetic reactivation of tumor suppressor genes by a novel small-molecule inhibitor of human DNA methyltransferases. *Cancer Res* 65:6305–6311. doi:10.1158/0008-5472.CAN-04-2957
46. Stach D, Schmitz OJ, Stilgenbauer S, Benner A, Dohner H, Wiessler M, Lyko F (2003) Capillary electrophoretic analysis of genomic DNA methylation levels. *Nucleic Acids Res* 31:e2. doi:10.1093/nar/gng002
47. Irwin JJ, Shoichet BK (2005) ZINC—a free database of commercially available compounds for virtual screening. *J Chem Inf Model* 45:177–182. doi:10.1021/ci049714+
48. FILTER, version 2.0.2. OpenEye Scientific Software Inc., Santa Fe, NM. <http://www.eyesopen.com>. Accessed April 2010
49. LigPrep, version 2.2 (2005) Schrödinger, LLC, New York, NY
50. Xu Y, Johnson M (2001) Algorithm for naming molecular equivalence classes represented by labeled pseudographs. *J Chem Inf Comput Sci* 41:181–185. doi:10.1021/ci0003911
51. Xu YJ, Johnson M (2002) Using molecular equivalence numbers to visually explore structural features that distinguish chemical libraries. *J Chem Inf Comput Sci* 42:912–926. doi:10.1021/ci0255351
52. Xu J (2002) A new approach to finding natural chemical structure classes. *J Med Chem* 45:5311–5320. doi:10.1021/jm010520k
53. Liu B, Lu A, Zhang L, Liu H, Liu Z, Zhou J (2004) New diversity criterion and database compression method. *Internet Electron J Mol Des* 3:143–149. <http://www.biochempress.com>
54. Bemis GW, Murcko MA (1996) The properties of known drugs. 1. Molecular frameworks. *J Med Chem* 39:2887–2893. doi:10.1021/jm9602928
55. Medina-Franco JL, Petit J, Maggiora GM (2006) Hierarchical strategy for identifying active chemotype classes in compound databases. *Chem Biol Drug Des* 67:395–408. doi:10.1111/j.1747-0285.2006.00397.x



56. Medina-Franco JL, Martínez-Mayorga K, Giulianotti MA, Houghten RA, Pinilla C (2008) Visualization of the chemical space in drug discovery. *Curr Comput Aided Drug Des* 4:322–333. doi:10.2174/157340908786786010
57. Singh N, Guha R, Giulianotti MA, Pinilla C, Houghten RA, Medina-Franco JL (2009) Chemoinformatic analysis of combinatorial libraries, drugs, natural products, and molecular libraries small molecule repository. *J Chem Inf Model* 49:1010–1024. doi:10.1021/ci800426u
58. Medina-Franco JL, Martínez-Mayorga K, Bender A, Scior T (2009) Scaffold diversity analysis of compound data sets using an entropy-based measure. *QSAR Comb Sci* 28:1551–1560. doi:10.1002/qsar.200960069
59. Molecular Operating Environment (MOE), version 2008.10. Chemical Computing Group Inc., Montreal, QC, Canada. <http://www.chemcomp.com>. Accessed April 2010
60. Glide, version 5.0 (2008) Schrödinger, LLC, New York, NY
61. Jones G, Willett P, Glen RC, Leach AR, Taylor R (1997) Development and validation of a genetic algorithm for flexible docking. *J Mol Biol* 267:727–748. doi:10.1006/jmbi.1996.0897
62. Huey R, Morris GM, Olson AJ, Goodsell DS (2007) A semiempirical free energy force field with charge-based desolvation. *J Comput Chem* 28:1145–1152. doi:10.1002/jcc.20634
63. Morris GM, Huey R, Lindstrom W, Sanner MF, Belew RK, Goodsell DS, Olson AJ (2009) AutoDock4 and AutoDockTools4: automated docking with selective receptor flexibility. *J Comput Chem* 30:2785–2791. doi:10.1002/jcc.21256
64. Gasteiger J, Marsili M (1980) Iterative partial equalization of orbital electronegativity—a rapid access to atomic charges. *Tetrahedron* 36:3219–3228. doi:10.1016/0040-4020(80)80168-2
65. Chuang JC, Yoo CB, Kwan JM, Li TWH, Liang GN, Yang AS, Jones PA (2005) Comparison of biological effects of non-nucleoside DNA methylation inhibitors versus 5-aza-2'-deoxycytidine. *Mol Cancer Ther* 4:1515–1520. doi:10.1158/1535-7163.MCT-05-0172
66. Stresemann C, Brueckner B, Musch T, Stopper H, Lyko F (2006) Functional diversity of DNA methyltransferase inhibitors in human cancer cell lines. *Cancer Res* 66:2794–2800. doi:10.1158/0008-5472.CAN-05-2821
67. Wishart DS, Knox C, Guo AC, Cheng D, Shrivastava S, Tzur D, Gautam B, Hassanali M (2008) DrugBank: a knowledgebase for drugs, drug actions and drug targets. *Nucleic Acids Res* 36:D901–D906. doi:10.1093/nar/gkm958
68. Charifson PS, Walters WP (2002) Filtering databases and chemical libraries. *J Comput Aided Mol Des* 16:311–323. doi:10.1023/A:1020829519597
69. Talevi A, Gavernet L, Bruno-Blanch LE (2009) Combined virtual screening strategies. *Curr Comput Aided Drug Des* 5:23–37. doi:10.2174/157340909787580854
70. Musa MA, Cooperwood JS, Khan MOF (2008) A review of coumarin derivatives in pharmacotherapy of breast cancer. *Curr Med Chem* 15:2664–2679
71. Wu L, Wang X, Xu W, Farzaneh F, Xu R (2009) The structure and pharmacological functions of coumarins and their derivatives. *Curr Med Chem* 16: 4236–4260. doi:10.2174/092986709789578187
72. CRC Dictionary of Natural Products. <http://www.crcpress.com/>. Accessed April 2010
73. Drug Discovery Portal. <http://www.ddp.strath.ac.uk/>. Accessed April 2010